ACTA PHYSIOLOGICA

Acta Physiol 2011, **202**, 241–251

Extracellular nucleotides affect pericyte-mediated regulation of rat *in situ* vasa recta diameter

C. Crawford,[1,*] T. M. Kennedy-Lydon,[1,*] H. Callaghan,[1] C. Sprott,[1] R. L. Simmons,[1] L. Sawbridge,[1] H. M. Syme,[2] R. J. Unwin,[3] S. S. P. Wildman[1,†] and C. M. Peppiatt-Wildman[1,†]

1 *Urinary System Physiology Unit, Department of Veterinary Basic Sciences, Royal Veterinary College, London, UK*

2 *Department of Veterinary Clinical Sciences, Royal Veterinary College, London, UK*

3 *Centre for Nephrology, Royal Free Hospital Medical School, UCL, London, UK*

Received 13 December 2010, revision requested 20 February 2011, revision received 12 April 2011, accepted 12 April 2011

Correspondence: Dr C. M. Peppiatt-Wildman, Urinary System Physiology Unit, Department of Veterinary Basic Sciences, Royal Veterinary College, Royal College Street, London NW1 0TU, UK.
E-mail: cpeppiattwildman@rvc.ac.uk

*These authors contributed equally to the work.

†These authors are joint senior authors.

Abstract

Aim: We hypothesized that extracellular nucleotides, established as being released from renal tubular epithelial cells, act at pericytes to regulate vasa recta capillary diameter.

Methods: A rat live kidney slice model and video imaging techniques were used to investigate the effects of extracellular nucleotides on *in situ* (sub-surface) vasa recta diameter at pericyte and non-pericyte sites. In addition, RT-qPCR was used to quantify P2 receptor mRNA expression in isolated vasa recta.

Results: Extracellular ATP, UTP, benzylbenzyl ATP (BzATP) or 2-methylthioATP (2meSATP) evoked a significantly greater vasoconstriction of sub-surface vasa recta at pericytes than at non-pericyte sites. The rank order of agonist potency was BzATP = 2meSATP > ATP = UTP. The vasoconstriction evoked at pericyte sites by ATP was significantly attenuated by the P2 receptor antagonists suramin, pyridoxal phosphate-6-azo(benzene-2,4-disulfonic acid) (PPADS) or Reactive Blue-2 (RB-2). UTP-evoked vasoconstriction at pericytes was attenuated by suramin or RB-2 but not PPADS. Interestingly, suramin or PPADS, when applied in the absence of a P2 receptor agonist, evoked a weak but significant vasoconstriction of vasa recta at pericyte sites, suggesting tonic vasodilation by nucleotides. Significant levels of $P2X_{1,\ 3\ \mathrm{and}\ 7}$ and $P2Y_{4\ \mathrm{and}\ 6}$ receptor mRNA were detected in vasa recta.

Conclusion: Extracellular nucleotides act at pericytes to cause vasoconstriction of *in situ* vasa recta. Pharmacological characterization, supported by RT-qPCR data, suggests that $P2X_{1\ \mathrm{and}\ 7}$ and $P2Y_4$ receptors mediate nucleotide-evoked vasoconstriction of vasa recta by pericytes. We propose that nucleotides released from renal tubular epithelial cells, in close proximity to vasa recta capillaries, are key in regulating renal medullary blood flow.

Keywords ATP, P2 receptor, purinergic, purinoceptor, renal blood flow, Rouget cell.

In 1929, the physiologist and Nobel laureate August Krogh proposed that pericytes, smooth muscle-like contractile cells of capillaries, regulate vessel diameter (Krogh 1929). Pericytes, consisting of a cell body and several long claw-like processes that wrap around vessels, have since been identified at regular intervals along capillaries in almost all organs and tissues in a wide range of species (Sims 1986). The density of

© 2011 The Authors

pericytes varies between tissue types, with the most dense coverage so far being reported for capillaries of the central nervous system (CNS), skeletal and cardiac muscle, and the medullary region of the kidney (Tilton *et al.* 1979, Frank *et al.* 1987, Shepro & Morel 1993).

Interestingly, renal medulla blood flow (i.e. blood flow through U-shaped 'vasa recta' capillaries that descend into the medulla and then ascend into the renal cortex in bundles with loop of Henlé and collecting duct tubules; vasa recta being a focus of this investigation) can be altered independently of changes in total renal blood flow (O'Connor *et al.* 2006), although the mechanism(s) by which medullary blood flow is controlled remains poorly understood. It has been proposed that changes in the descending vasa recta (DVR) diameter because of pericyte contraction and relaxation can determine medullary blood flow and distribution in relation to changes in tubular transport and the oxygen demands of tubular epithelial cells (Pallone & Silldorff 2001). Furthermore, damage to pericytes in the renal medulla has recently been proposed as a cause of kidney fibrosis and subsequent renal failure (Lin *et al.* 2008).

It has long been known that extracellular nucleotides and nucleosides acting through P2 and P1 purinoceptors, respectively, have a profound effect on the vasculature, including the renal vasculature, and are important in maintaining vascular tone (Burnstock & Knight 2004). In very general terms, nucleotides cause either vasoconstriction via smooth muscle contraction or vasodilation via nitric oxide release from endothelial cells, and nucleosides cause vasodilation via actions at both smooth muscle and endothelial cells (Fredholm *et al.* 2007, Erlinge & Burnstock 2008). Of particular relevance to this study, extracellular adenosine has been shown to have a concentration-dependent effect at renal pericytes on isolated DVR, causing constriction at low concentrations and dilation at higher concentrations (Silldorff *et al.* 1996). The effect of extracellular nucleotides on vasa recta diameter, at pericyte and non-pericyte sites, has yet to be determined, although most apposite investigations have demonstrated that extracellular ATP or UTP can cause constriction of CNS capillaries specifically at pericyte sites (Kawamura *et al.* 2003, Peppiatt *et al.* 2006).

It is known that vasa recta are in close proximity to renal tubules, isolated vasa recta diameter is altered by extracellular adenosine (Silldorff *et al.* 1996) and pericytes in the CNS are sensitive to extracellular nucleotides (Kawamura *et al.* 2003, Peppiatt *et al.* 2006). It has also been demonstrated that extracellular ATP, UTP and adenosine are released from the renal epithelium in response to both cell swelling and hypoxia, and adenosine is a product of ATP breakdown by ecto-ATPases (Jans *et al.* 2002, Schwiebert & Zsembery 2003, Praetorius *et al.* 2005). Together, this suggests the possibility of tubulovascular cross-talk in the renal medulla, whereby tubular cell activity (e.g. solute and water transport), or hypoxia affecting renal epithelium, may cause an alteration in vasa recta diameter, and therefore medullary blood flow, via the actions of extracellular nucleotides at vasa recta pericytes. As a first step in understanding tubulovascular cross-talk between medullary renal tubules and renal medulla microvasculature, we have investigated the direct effect of extracellular nucleotides, known to be released from tubular epithelium, on *in situ* vasa recta capillaries using a novel live kidney slice model.

Materials and methods

Animals

Animal experiments were conducted in accordance with United Kingdom Home Office Scientific Procedures Act (1986). Adult male Sprague–Dawley rats (250–300 g) were purchased from Charles River Laboratories (Margate, Kent, UK) and housed for a minimum period of 3 days before being used in experiments. Animals were fed on a standard adult rat maintenance chow and exposed to a 12 : 12-h light : dark cycle. Prior to experimentation, animals were killed by cervical dislocation.

Tissue slices

Kidneys were rapidly removed, decapsulated and placed in ice-cold physiological saline solution (PSS) bubbled with 95% O_2/5% CO_2. PSS contained (mm): NaCl (100), KCl (5), NaH_2PO_4 (0.24), Na_2HPO_4 (0.96), Na acetate (10), $CaCl_2$ (1), $MgSO_4$ (1.2), glucose (5), $NaHCO_3$ (25), pyruvate (5), and pH was adjusted to 7.4 using 10 m NaOH. A single kidney was secured to the slicing block of a vibratome slicer (Vibroslice model MA752; Campden Instruments, Loughborough, UK) and submerged in a bath of ice-cold oxygenated PSS. The outer cortical dome region of the kidney was removed to expose the top of the renal medulla and serial 200 μm-thick coronal kidney slices were cut. Slices were collected and maintained for up to 3 h at room temperature, in a holding chamber containing oxygenated PSS; we have previously reported that kidney slices remain viable for over 3 h (Crawford *et al.* 2009).

Immunohistochemistry

Live kidney slices were incubated with Alexa Fluor 488-conjugated isolectin B4 (IB_4; Invitrogen, Paisley, UK) – a marker for α-D-galactosyl residues – to identify the vasa recta capillaries (Fig. S1). IB_4 (50 $\mu g\ mL^{-1}$) was

© 2011 The Authors

Acta Physiologica © 2011 Scandinavian Physiological Society, doi: 10.1111/j.1748-1716.2011.02310.x

17481716, 2011, 3, Downloaded from https://onlinelibrary.wiley.com/doi/10.1111/j.1748-1716.2011.02310.x by Northeastern Universitaet, Wiley Online Library on [10/07/2023]. See the Terms and Conditions (https://onlinelibrary.wiley.com/terms-and-conditions) on Wiley Online Library for rules of use; OA articles are governed by the applicable Creative Commons License

prepared in PSS bubbled with 95% O_2/5% CO_2; slices were incubated with IB_4 for 45 min, washed with PSS and subsequently fixed using 4% paraformaldehyde (PFA). Fixed kidney slices were then incubated for 16 h with anti-neural-glial 2 (NG2) polyclonal antibody (Millipore UK, Watford, UK). NG2 was used previously to identify pericytes in the CNS (Peppiatt *et al.* 2006) and was probed with an Alexa Fluor 555-conjugated donkey anti-rabbit secondary antibody (Invitrogen; Fig. S1). Kidney slices were mounted using Citiflour (Agar Scientific, Stanstead, UK) and the medulla of the fixed slices was imaged using a Zeiss LSM 510 laser scanning confocal microscope (Carl Zeiss, Welwyn Garden City, UK). Alexa 488-conjugated IB_4 was excited at 488 nm and Alexa Fluor 555-conjugated secondary antibody was excited at 543 nm. Emitted light was collected with the following filters: long-pass 560 nm (Alexa Fluor 555) and band-pass 505–550 nm (IB_4).

Functional experiments and video analysis

A single kidney slice was secured in an open-bath chamber using a purpose-built platinum slice anchor, and then transferred to the stage of an upright Olympus microscope (model BX51WI, Olympus Southend-on-Sea, UK). The tissue slice was continually superfused (approx. 2.5 mL min^{-1}, 1.25 mL bath volume) with oxygenated PSS maintained at 20–23 °C. Differential interference contrast images of pericytes on subsurface vasa recta capillaries (i.e. approx. 50 μm below the surface of the tissue; identified by their 'bump on a log' morphology; Peppiatt *et al.* 2006), as seen in confocal images of anti-NG2-labelled pericytes (Fig. S1), were captured through a 63× water immersion objective. Real-time video images of changes in vasa recta diameter were collected every 1 s by an attached Rolera XR CCD camera (Qimaging, Surrey, Canada), and recorded using Image Pro Software (Media Cybernetics, Maidenhead, UK).

Live kidney slices were superfused with purinoceptor agonists [ATP, UTP, benzylbenzyl ATP (BzATP), 2-methylthioATP (2meSATP) or adenosine] and antagonists [suramin, Reactive Blue-2 [RB-2] or pyridoxal phosphate-6-azo(benzene-2,4-disulfonic acid) (PPADS)]. All compounds were purchased from Sigma-Aldrich (Poole, UK), and working solutions were prepared in oxygenated PSS. In experiments to determine the activity of purinoceptor agonists on vasa recta diameter, kidney slices were superfused with oxygenated PSS alone for 70 s to establish a baseline vessel diameter at the pericyte and non-pericyte site. Slices were then exposed to a chosen agonist (for approx. 250 s) and then subjected to a PSS-wash to assess reversibility. Similar experiments were performed to assess whether P2 receptor antagonists, in the absence of an agonist, affected vasa recta diameter; in these experiments the chosen antagonist was applied for 300 s. In experiments to determine the effect of P2 receptor antagonists, or the ecto-nucleotidase inhibitor ARL 67156, on ATP- or UTP-evoked changes in vasa recta diameter, kidney slices were superfused with oxygenated PSS alone for 70 s to establish a baseline vessel diameter at the pericyte and non-pericyte site, then slices were pre-incubated with a P2 receptor antagonist (or ARL 67156; for 300 s), followed by superfusion of antagonist (or ARL 67156) in the presence of an agonist for a further approx. 250 s. Subsequently, the slices were superfused with the agonist alone for approx. 250 s, before a return to the PSS control solution. Analysis of video recordings of drug-evoked changes in capillary diameter was carried out using the public domain software IMAGE J (NIH; http://rsb.info.nih.gov). For each experiment, a pericyte site and non-pericyte site were identified on a single vasa recta capillary. The diameter of the vasa recta at both these locations was measured every five frames for the duration of the experiment (one frame = 1 s). Each capillary acted as its own control, where an average of the first five measurements was taken to represent the resting diameter value (i.e. 100%) for the selected pericyte and non-pericyte sites. All subsequent diameter measurements at both sites were calculated as a percentage of the corresponding resting diameter value as previously described (Peppiatt *et al.* 2006).

Isolation of vasa recta

Kidneys were obtained as above. Vasa recta were isolated using a protocol developed by Pallone & Huang (2002). In brief, the medulla was cut free from the cortex and then cut into small segments. Each segment was placed in a 34-mm Petri dish containing 2 mL of $CaCl_2$-free PSS containing collagenase type 1A (0.45 mg mL^{-1}), protease XIV (0.4 mg mL^{-1}) and albumin (1 mg mL^{-1}). Tissue segments were incubated at 37 °C for 25 min and then transferred back to ice-cold oxygenated PSS solution. Segments were teased apart to isolate vasa recta which were subsequently stored in RNAlater (Ambion Applied Biosystems, Warrington, UK) until required for RNA extraction.

RNA extraction from isolated vasa recta

Isolated vasa recta were homogenized in Tri-Reagent (Sigma-Aldrich), then freeze–thawed in liquid nitrogen followed by chloroform extraction and ethanol precipitation. Precipitated RNA was loaded onto Qiagen RNeasy columns (Qiagen, Crawley, UK) for DNase treatment and further purification. Total RNA was

© 2011 The Authors

17481716, 2011, 3, Downloaded from https://onlinelibrary.wiley.com/doi/10.1111/j.1748-1716.2011.02310.x by Northeastern Universitaet, Wiley Online Library on [10/07/2023]. See the Terms and Conditions (https://onlinelibrary.wiley.com/terms-and-conditions) on Wiley Online Library for rules of use; OA articles are governed by the applicable Creative Commons License

eluted with RNase-free water before spectrophotometric measurement of concentration and purity using Nano N-1000 system (Nanodrop Technologies, Wilmington, DE, USA).

RT-qPCR

Total RNA (5 ng) from each sample was reverse transcribed in a 20-μL reaction volume using the One-Step Quantitect Reverse Transcription kit (Qiagen) according to the manufacturer's instructions. All primers were manufactured by Eurofins MWG Operon (London, UK) (for sequences and accession numbers, see Table S1). Using SyBR green detection (Qiagen), RT-PCR was performed on a Chromo-4 thermal cycler (Bio-Rad Laboratories, Hemel Hempstead, UK) with 1 μL total RNA. Chromo-4 thermal cycler software was used to determine the relative concentrations of the target amplicons using a standard curve. This standard curve was created with duplicate serial dilutions of standard DNA (target sequence of interest) over 12 logarithmic orders. In addition, the standard curve was used to verify the linearity of amplification of each transcript; $r > 0.99$ in all cases. The relative concentrations of each target are expressed as a ratio to the housekeeping gene, glyceraldehyde 3-phosphate dehydrogenase (GAPDH). All PCR products were checked for specificity and purity from a melting curve profile, created after each run, by the thermal cycler software. Homology of the PCR products was further checked for size by agarose gel electrophoresis.

Statistics

All data are presented as mean values ± SEM; n numbers displayed represent number of pericytes (one pericyte and non-pericyte site per kidney slice) and not animals, as variation observed here and in similar CNS studies (Peppiatt *et al.* 2006) occurred between pericytes and not animals. All experiments were performed in at least three different animals. Statistical evaluation was performed with Instat (v2.05a; GraphPad Software, San Diego, CA, USA). When two groups were compared, Student's *t*-test (two-tailed, paired or unpaired where appropriate) was used. For multiple comparisons, one-way ANOVA was performed followed by Bonferroni's multiple comparison tests. A value of $P < 0.05$ was considered significant.

Results

Identification of in situ *vasa recta pericytes*

Immunohistochemical labelling of pericytes (anti-NG2) and *in situ* vasa recta capillaries (IB_4) demonstrated the presence of pericytes at regular intervals along vasa recta capillaries in the medulla (Fig. S1). Confocal images of anti-NG2-labelled pericytes were used to determine the average distance between pericyte somas along vasa recta capillaries (15.6 ± 1.8 μm, $n = 20$) and the density of pericytes per 100 μm^2 (10.8 ± 0.7, $n = 20$).

Effects of purinoceptor agonists on in situ *pericyte activity*

Purinoceptor agonists (ATP, UTP, BzATP, 2meSATP and adenosine) were tested for their ability to alter the diameter of subsurface vasa recta at both pericyte and non-pericyte sites in live kidney slices.

Superfusion (approx. 250 s) of ATP (100 μM) caused a reversible vasoconstriction of vasa recta primarily at pericyte sites (Fig. 1a; Movie S1). Vasoconstriction was significantly greater at pericyte sites (19.4 ± 2.8%, $n = 11$) than at non-pericyte sites (3.3 ± 2.9%, $n = 11$; $P < 0.01$) (Fig. 1b). Similarly, superfusion of UTP (100 μM), BzATP (100 μM) and 2meSATP (100 μM) caused a significantly greater vasoconstriction of vasa recta at pericyte sites (12.2 ± 1.2%, $n = 5$; 15.9 ± 2.1%, $n = 7$; 12.1 ± 2.3%, $n = 4$ respectively) than at non-pericyte sites (2.9 ± 1.5%, $n = 5$; 3.0 ± 1.2%, $n = 7$; 2.6 ± 0.5%, $n = 4$ respectively; $P < 0.01$ in all cases) (Fig. 2a); agonist-evoked vasoconstriction was reversible on washout in all cases. Furthermore, in all experiments, vasa recta diameter at pericyte sites returned towards its original diameter in the presence of the agonist (at 100 μM) (i.e. desensitization occurred).

The degree of vasoconstriction was dependent on the concentration of P2 receptor agonist (Fig. 2b). Both BzATP and 2meSATP evoked vasoconstriction at 10 μM, whereas for ATP and UTP a concentration of 100 μM was necessary to elicit a vasoactive effect (Fig. 2b). The greatest degree of vasoconstriction was evoked by 10 μM BzATP (20.2 ± 2.5% decrease in resting vessel diameter; $n = 6$) and 100 μM ATP (19.4 ± 2.8% decrease in resting vessel diameter; $n = 11$), whereas the greatest degree of vasoconstriction caused by 2meSATP (12.1 ± 2.3% decrease in resting vessel diameter; $n = 4$; 100 μM) and UTP (12.2 ± 1.2% decrease in resting vessel diameter; $n = 5$; 100 μM) was approx. 2-fold less (Fig. 2b).

Superfusion (approx. 250 s) of adenosine (10 μM) caused a reversible vasodilation of vasa recta primarily at pericyte sites (Fig. 3a). Vasodilation was significantly greater at pericyte sites (7.7 ± 1.0%, $n = 6$) than at non-pericyte sites (1.8 ± 0.8%, $n = 6$; $P < 0.01$) (Fig. 3b). In contrast to the nucleotide-evoked changes in vessel diameter, the adenosine-evoked vasodilation did not desensitize. Higher concentrations of adenosine (100 μM) failed to evoke a greater degree of vasodilation

© 2011 The Authors

Acta Physiologica © 2011 Scandinavian Physiological Society, doi: 10.1111/j.1748-1716.2011.02310.x

1748176, 2011, 3, Downloaded from https://onlinelibrary.wiley.com/doi/10.1111/j.1748-1716.2011.02310.x by Northeastern Universitaet, Wiley Online Library on [10/07/2023]. See the Terms and Conditions (https://onlinelibrary.wiley.com/terms-and-conditions) on Wiley Online Library for rules of use; OA articles are governed by the applicable Creative Commons License

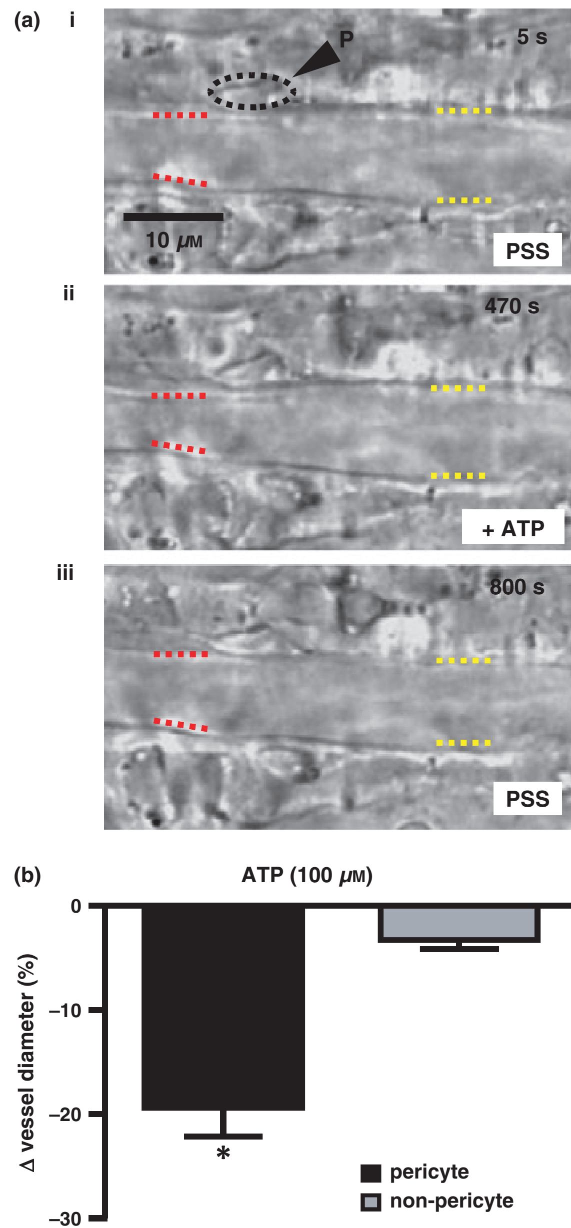

Figure 1 Differential interference contrast imaging of pericyte-mediated constriction of *in situ* vasa recta capillaries by ATP (100 μM). Images of vasa recta in (a) are taken from a time series experiment in which kidney slices were exposed to ATP (100 μM). (i) A typical field of view of vasa recta under control conditions [physiological saline solution (PSS)]; the pericyte is highlighted by black dashed lines and marked by an arrowhead. (ii) Vasa recta constrict at pericyte sites during exposure to ATP and (iii) vasa recta diameter returns towards original diameter when ATP is removed. Vessel diameter was measured every 5 s throughout the experiment at a pericyte site (red dashed lines) and a non-pericyte site (yellow dashed lines). Bar graph in (b) is mean data showing percentage change in vessel diameter at pericyte sites (black bar) and non-pericyte sites (grey bar). ATP (100 μM) evoked a significantly greater constriction of vasa recta at pericyte sites than at non-pericyte sites (mean ± SEM, $^*P < 0.01$, $n = 11$).

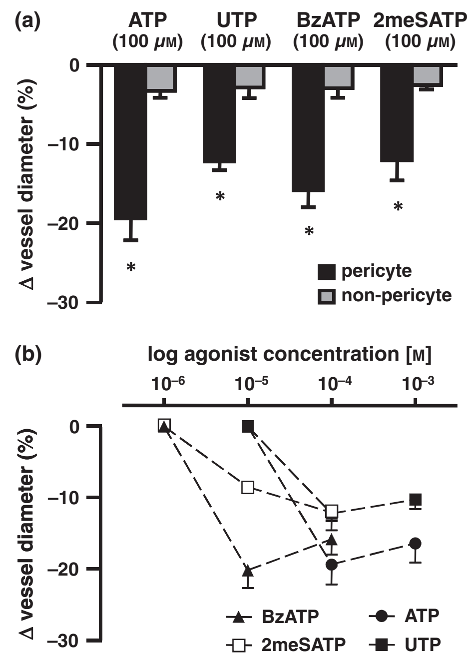

Figure 2 The effect of P2 receptor agonists on *in situ* vasa recta diameter. Bar graph in (a) shows P2 receptor agonists ATP, UTP, BzATP and 2meSATP evoked a significantly greater constriction of vasa recta at pericyte sites (black bars) compared with non-pericyte sites (grey bars); data are mean SEM, $^*P < 0.01$, $n > 5$. Line graph in (b) shows the concentration-dependent effect of the agonist-evoked change in vasa recta diameter at pericyte sites for all P2 receptor agonists shown in (a); data are mean ± SEM, $n > 5$.

and lower concentrations (100 nM–1 μM) were without vasoactivity (data not shown).

Effects of P2 receptor antagonists on agonist-evoked vasoconstriction by in situ *pericytes*

P2 purinoceptor antagonists (suramin, PPADS and RB-2) were tested for their ability to inhibit ATP- or UTP-evoked changes in the diameter of subsurface vasa recta at pericyte sites in live kidney slices.

Pre-incubation (300 s) of kidney slices with suramin (100 μM), PPADS (100 μM) or RB-2 (100 μM) significantly attenuated ATP-evoked vasoconstriction of vasa recta at pericyte sites (by 54.7 ± 13.1%, $n = 7$; 74.9 ± 5.0%, $n = 7$; 74.0 ± 5.7%, $n = 7$ respectively; $P < 0.01$ in all cases) (Fig. 4a). No further vasoconstriction was observed when slices were pre-incubated with suramin and RB-2 in combination (data not shown). In contrast, only suramin (100 μM) and RB-2 (100 μM) significantly inhibited UTP-evoked vasoconstriction of vasa recta at pericyte sites (by 49.3 ± 11.7%, $n = 6$; 26.6 ± 10.2%, $n = 8$ respectively; $P < 0.01$ in all cases); PPADS (100 μM) was without effect (Fig. 4b). When applied to kidney slices alone,

© 2011 The Authors

17481716, 2011, 3, Downloaded from https://onlinelibrary.wiley.com/doi/10.1111/j.1748-1716.2011.02310.x by Northeastern Universitaet, Wiley Online Library on [10/07/2023]. See the Terms and Conditions (https://onlinelibrary.wiley.com/terms-and-conditions) on Wiley Online Library for rules of use; OA articles are governed by the applicable Creative Commons License

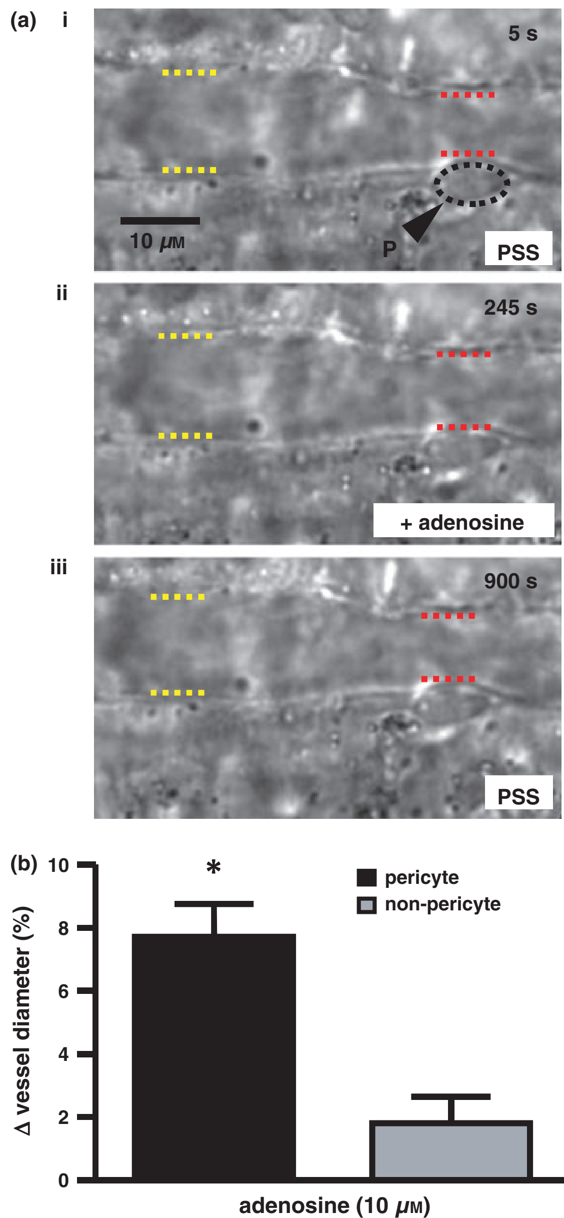

Figure 3 Differential interference contrast imaging of adenosine evoked dilation of *in situ* vasa recta. Images of vasa recta in (a) are taken from a time series experiment in which kidney slices were exposed to adenosine (10 μM). (i) A typical field of view of vasa recta under control conditions [physiological saline solution (PSS)]; the pericyte is highlighted by black dashed lines and marked by an arrowhead. (ii) Vasa recta dilate at pericyte sites during exposure to adenosine and (iii) vasa recta diameter returns towards original diameter when adenosine is removed. Vessel diameter was measured every 5 s throughout the experiment at a pericyte site (red dashed lines) and a non-pericyte site (yellow dashed lines). Bar graph in (b) is mean data showing percentage change in vessel diameter at pericyte sites (black bar) and non-pericyte sites (grey bar). Adensoine (10 μM) evoked a significantly greater dilation of vasa recta at pericyte sites than at non-pericyte sites (mean SEM, $*P < 0.01$, $n = 6$).

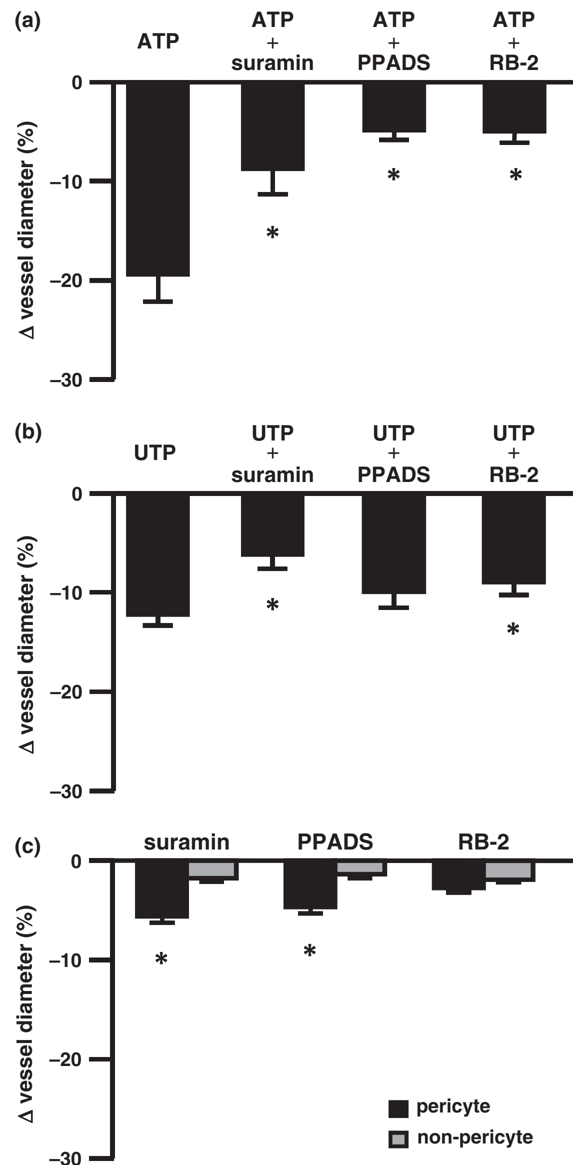

Figure 4 The effect of P2 receptor antagonists on ATP and UTP-evoked constriction of *in situ* vasa recta. Bar graph in (a) shows P2 receptor antagonists suramin (100 μM), PPADS (100 μM) and RB-2 (100 μM) significantly attenuated the ATP (100 μM)-evoked constriction of vasa recta at pericyte sites. Bar graph in (b) shows the UTP (100 μM)-evoked constriction of vasa recta at pericyte sites was significantly attenuated by suramin (100 μM) and RB-2 (100 μM), but not by PPADS (100 μM). Bar graph in (c) shows the percentage change in vasa recta diameter in response to application of P2 receptor antagonists alone. Suramin and PPADS, but not RB-2, evoked a significantly greater vasoconstriction of vasa recta at pericyte sites than at non-pericyte sites. In (a–c), data are mean ± SEM, $*P < 0.01$, $n > 6$.

suramin (100 μM; applied for 250 s) and PPADS (100 μM; applied for 200 s) caused a weak, reversible vasoconstriction of vasa recta that was significantly

© 2011 The Authors
Acta Physiologica © 2011 Scandinavian Physiological Society, doi: 10.1111/j.1748-1716.2011.02310.x

17481716, 2011, 3, Downloaded from https://onlinelibrary.wiley.com/doi/10.1111/j.1748-1716.2011.02310.x by Northeastern Universitaet, Wiley Online Library on [10/07/2023]. See the Terms and Conditions (https://onlinelibrary.wiley.com/terms-and-conditions) on Wiley Online Library for rules of use; OA articles are governed by the applicable Creative Commons License

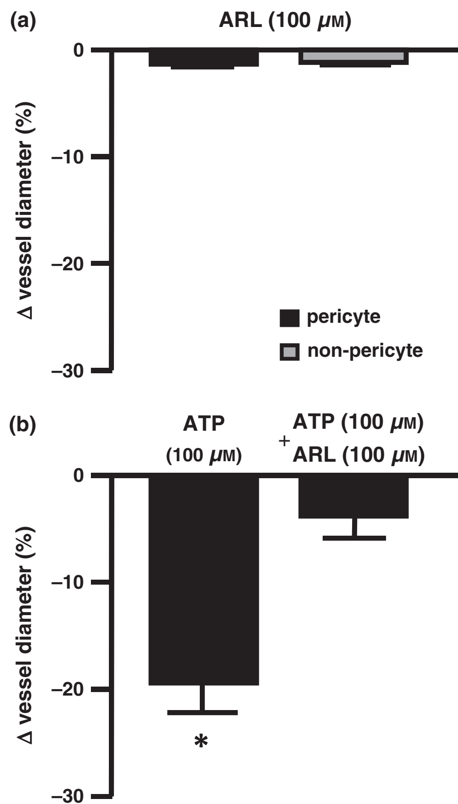

Figure 5 Effect of ARL 67156 on ATP-mediated vasoconstriction of *in situ* vasa recta. Bar graph in (a) shows that ARL 67156 did not significantly alter vasa recta diameter at pericyte sites compared with non-pericyte sites. Bar graph in (b) shows co-application of ARL 67156 (100 μM) and ATP (100 μM) significantly attenuated the ATP (100 μM)-evoked constriction of vasa recta at pericyte sites. In (a) and (b), data are mean SEM, $*P < 0.01$, $n = 5$.

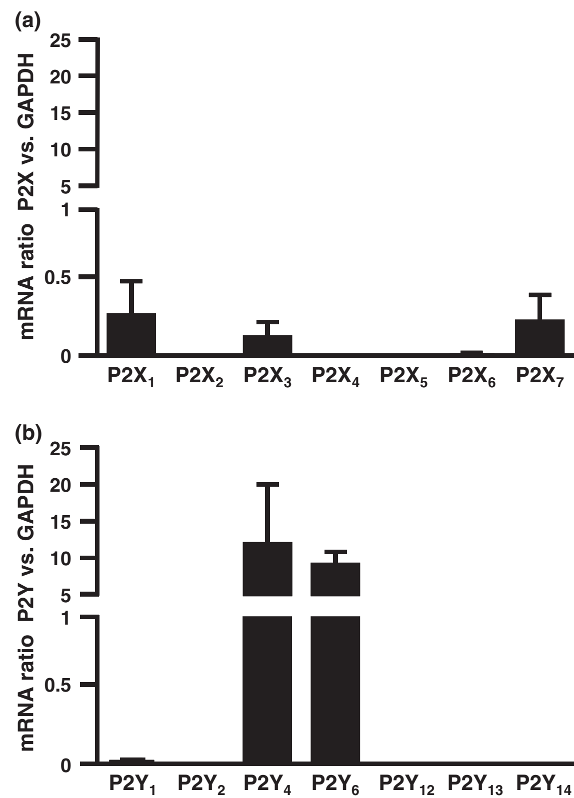

Figure 6 P2 receptor mRNA expression levels in isolated vasa recta. (a, b) show P2X and P2Y receptor mRNA expression levels, respectively, in isolated vasa recta. Data are expressed as a ratio of P2 receptor gene to the constitutively expressed housekeeping gene, GAPDH (mean ± SEM, $n = 6$).

greater at pericyte sites (5.6 ± 0.6%, $n = 13$; 4.7 ± 0.6%, $n = 13$ respectively) than at non-pericyte sites (1.8 ± 0.4%, $n = 13$; 1.4 ± 0.4%, $n = 13$ respectively; $P < 0.01$ in all cases) (Fig. 4c), suggesting tonic vasodilation by nucleotides.

Effects of ARL 67156 on ATP-evoked vasoconstriction by in situ *pericytes*

To further investigate the apparent tonic P2 receptor-mediated vasodilation, blocked by suramin or PPADS (Fig. 4c), we tested the effect of the ecto-nucleotidase inhibitor ARL 67156 alone (to further reveal tonic vasodilation) and in the presence of ATP (to further reveal stimulated vasoconstriction).

ARL 67156 (100 μM; applied for 250 s) did not alter vasa recta diameter at either pericyte or non-pericyte sites (Fig. 5a). Yet, ARL 67156 (100 μM), when co-applied with ATP (100 μM), almost abolished ATP-evoked vasoconstriction of vasa recta at pericyte sites (by 80.2 ± 10.5%, $n = 5$) (Fig. 5b). ARL 67156 did not significantly alter vasa recta diameter at non-pericyte sites in the presence of ATP (data not shown).

mRNA levels of P2 receptor in vasa recta

To quantify the relative abundance of P2 receptor mRNA in isolated vasa recta (i.e. endothelial cells and pericytes), we calculated a ratio to a constitutively expressed housekeeping gene (GAPDH). No suitable primer was available for the $P2Y_{11}$ receptor subtype.

We failed to detect significant levels (i.e. levels >0.1 arbitrary unit) of $P2X_{2,\ 4,\ 5\ \text{and}\ 6}$ and $P2Y_{1,\ 2,\ 12,\ 13\ \text{and}\ 14}$ mRNA ($n = 6$; Fig. 6a,b). In contrast, significant amounts of mRNA were detected for $P2X_{1,\ 3\ \text{and}\ 7}$ and $P2Y_{4\ \text{and}\ 6}$ ($n = 6$; Fig. 6a,b). The rank order of mRNA abundance for P2 receptors in rat isolated vasa recta was $P2Y_4=P2Y_6>>P2X_1=P2X_3=P2X_7$, where abundance of $P2Y_{4\ \text{and}\ 6}$ was 40-fold greater.

Discussion

The main findings of this investigation, using a novel live kidney slice model, revealed that pericytes occur at

© 2011 The Authors

17481716, 2011, 3, Downloaded from https://onlinelibrary.wiley.com/doi/10.1111/j.1748-1716.2011.02310.x by Northeastern Universitaet, Wiley Online Library on [10/07/2023]. See the Terms and Conditions (https://onlinelibrary.wiley.com/terms-and-conditions) on Wiley Online Library for rules of use; OA articles are governed by the applicable Creative Commons License

regular intervals along medullary vasa recta and that extracellular nucleotides act at pericytes to cause vasoconstriction of *in situ* vasa recta. More specifically, we present evidence that (i) P2 receptors mediate nucleotide-evoked vasoconstriction by pericytes and (ii) endogenous nucleotides mediate tonic vasodilation by pericytes. The latter finding suggests that nucleotides have a concentration-dependent effect at renal pericytes, causing vasodilation at low concentrations and vasoconstriction at high concentrations.

The sources of extracellular nucleotides?

It is perhaps prudent to begin this discussion by addressing the potential sources of endogenous extracellular nucleotides that may act on renal pericytes, thereby indirectly addressing the physiological significance of this investigation. It is widely accepted that ATP, and other nucleotides, are secreted from almost all cell types by a variety of mechanisms that are not yet fully resolved (Burnstock & Knight 2004). Probable sources of extracellular nucleotides acting on pericytes of the vasa recta are released from: (i) varicosities on sympathetic nerves innervating the renal medulla (Loesch *et al.* 2009), (ii) endothelial cells of the vasa recta in response to sheer stress and/or hypoxia (Bodin *et al.* 1991), (iii) blood cells (especially intraluminal red blood cells in response to mechanical deformation during vessel constriction) (Sprague *et al.* 1996) and (iv) epithelial cells, in close apposition to vasa recta (i.e. principal and/or intercalated cells of the medullary collecting duct, and tubular cells of the loop of Henlé), in response to mechanical stress (including sheer stress), increases in cell volume or hypoxia (Jans *et al.* 2002, Praetorius *et al.* 2005).

Given that the kidney is poorly innervated, compared with other organs, and the renal medulla is an especially hypoxic environment (Epstein 1985), it is likely that the major sources of extracellular nucleotides are from endothelial, epithelial and red blood cells. It is interesting to note that extracellular nucleotides, acting as autocrine or paracrine factors, are inhibitors of renal epithelial transport processes in the medulla, and these processes are intimately linked to medullary blood supply for cell survival and completion of renal solute reabsorption/secretion, suggesting tubulovascular cross-talk must occur (Seldin & Geibisch 2008).

P2 receptor-mediated vasoconstriction of vasa recta by pericytes

It has already been established that activation of P2 receptors by extracellular nucleotides can cause vasoconstriction of microvasculature by pericytes (Das *et al.* 1988, Metea & Newman 2006, Peppiatt *et al.* 2006), albeit using retina microvessels or cultured retinal pericytes. It is therefore perhaps surprising that extracellular nucleotides have previously been reported to have no effect on renal pericytes (Pallone & Silldorff 2001). Here, we demonstrate that exogenous application of ATP, and other nucleotides, causes vasoconstriction of *in situ* vasa recta, specifically at sites along the vessel where pericytes are located. The nucleotide-evoked vasoconstriction is concentration-dependent and blocked by P2 receptor antagonists. Taken together, we demonstrate that extracellular nucleotides act on P2 receptors expressed on pericytes to cause significant vasoconstriction (e.g. up to a 19% decrease in vessel diameter with ATP; Fig. 1b) of the vasa recta.

Interestingly, using Poiseuille's law, the ATP-evoked 19% decrease in vessel diameter we report here equates to a 2.3-fold increase in vasa recta resistance and thus a 57% decrease in blood flow (Peppiatt *et al.* 2006). It is noteworthy that a 19% decrease in vasa recta diameter suggests a decrease in vessel diameter from approx. 10 μm to approx. 8 μm, a diameter still adequate for red blood cells to travel through the vasa recta.

The experimental models used possibly explain the disparity between our study and that stating renal pericytes are insensitive to extracellular nucleotides (Pallone & Silldorff 2001). Here, we report findings using a novel kidney slice technique that allows the imaging of subsurface *in situ* vasa recta, whereas previous studies have used isolated vasa recta. It is well established that cell/tissue damage results in the release of nucleotides, and that P2 receptors desensitize in the continued presence of agonists, especially at high concentrations. The possibility exists that during the microdissection process to obtain isolated vasa recta, P2 receptors on pericytes are desensitized as a result of substantial tissue damage.

Maintenance of vasa recta tone by extracellular nucleotides

Interestingly, suramin or PPADS, but not RB-2, when applied in the absence of a P2 receptor agonist, evoked a weak but significant vasoconstriction of the vasa recta at pericyte sites (Fig. 4c). We propose that tonic release of extracellular nucleotides, acting at P2 receptors on pericytes, leads to pericyte relaxation and subsequent vasodilation, thus contributing to vasa recta tone.

This finding suggests a concentration-dependent role for extracellular nucleotides, whereby they cause dilation at low concentrations (i.e. basal release) and constriction at higher concentrations (i.e. stimulated release), both through their action at pericytes. This is in line with other vascular studies that show P2 receptors mediate both vasodilation and vasoconstriction (Dietrich *et al.* 1996, Horiuchi *et al.* 2001). A similar

© 2011 The Authors
Acta Physiologica © 2011 Scandinavian Physiological Society, doi: 10.1111/j.1748-1716.2011.02310.x

1748176, 2011, 3, Downloaded from https://onlinelibrary.wiley.com/doi/10.1111/j.1748-1716.2011.02310.x by Northeastern Universitaet, Wiley Online Library on [10/07/2023]. See the Terms and Conditions (https://onlinelibrary.wiley.com/terms-and-conditions) on Wiley Online Library for rules of use; OA articles are governed by the applicable Creative Commons License

17481716, 2011, 3, Downloaded from https://onlinelibrary.wiley.com/doi/10.1111/j.1748-1716.2011.02310.x by Northeastern Universitaet, Wiley Online Library on [10/07/2023]. See the Terms and Conditions (https://onlinelibrary.wiley.com/terms-and-conditions) on Wiley Online Library for rules of use; OA articles are governed by the applicable Creative Commons License

concentration-dependent effect at renal pericytes has been reported for adenosine, although in stark contrast, extracellular adenosine causes constriction at low concentrations and dilation at higher concentrations (Silldorff *et al.* 1996). Here, we report that extracellular adenosine (100 μM) causes pericyte-mediated vasodilation of the vasa recta (Fig. 3b), although we failed to see vasoconstriction at lower concentrations (100 nM). We acknowledge that in our investigation we did not test adenosine at low nM concentrations, which may account for this discrepancy. It is noteworthy that the concentration-dependent effect of adenosine is attributed to distinct P1 receptor subtypes/populations (Holz & Steinhausen 1987, Silldorff *et al.* 1996). Given that the P2 receptor antagonist RB-2, when applied in the absence of an agonist, did not effect vasa recta diameter (Fig. 4c), yet attenuated ATP- and UTP-evoked vasoconstriction by pericytes (Fig. 4a,b respectively), suggests that distinct subypes/populations of P2 receptors may be responsible for the concentration-dependent effects observed here.

As a final note in this section, we had hoped to provide further evidence for nucleotide-evoked regulation of vasa recta tone by applying the ecto-nucleotidase inhibitor ARL 67156, predicting that inhibition of basal nucleotide breakdown would further increase the degree of vasodilation. However, ARL 67156 had no effect when applied alone (Fig. 5a), and somewhat bafflingly attenuated ATP-evoked vasoconstriction (Fig. 5b). It is interesting to note that ARL 67156 has previously been demonstrated to act as a broad acting P2 receptor antagonist (Vassort 2001). It is possible therefore that ARL 67156 is in fact acting as an antagonist of P2 receptors expressed on pericytes, and in so doing is attenuating the vasoconstrictor action of ATP, by antagonizing the receptors on which ATP acts to cause constriction of the vasa recta.

P2 receptors in renal pericytes

We characterized molecularly the P2 receptors expressed in isolated vasa recta, which consist of epithelial cells, pericytes and presumably various types of blood cells. We demonstrated expression of $P2X_{1,\ 3\ \text{and}\ 7}$ and $P2Y_{4\ \text{and}\ 6}$ receptor mRNA (Fig. 6a,b). Our PCR findings are in broad accordance with many review articles that report $P2Y_{1,\ 2,\ 4\ \text{and}\ 12}$ receptor expression in endothelial cells, and $P2X_1$ and $P2Y_{2\ \text{and}\ 6}$ receptor expression in smooth muscle cells; however, it has become apparent to us that P2 receptor expression varies from one vessel to another depending on the type and location (Burnstock & Knight 2004).

By using a variety of P2 receptor agonists and antagonists (and taking account of our RT-qPCR findings), this study provides evidence for the involvement of both ionotropic P2X and metabotropic P2Y receptors in pericyte-mediated vasoconstriction of the vasa recta. We suggest that $P2X_{1\ \text{and}\ 7}$ and $P2Y_4$

Table 1 Pharmacological properties corresponding to P2 receptor subtypes identified in isolated rat vasa recta (including pericytes). P2 receptors were identified in our RT-qPCR studies. Information taken from Bogdanov *et al.* (1998), Wildman *et al.* (2002), King & Townsend-Nicholson (2003), Wildman *et al.* (2008)

	$P2X_1$	$P2X_3$	$P2X_6$	$P2X_7$	$P2Y_4$	$P2Y_6$	$P2Y_{11}$
ATP	Agonist	Agonist	–	Agonist	Agonist	i.a.	Agonist
UTP	Agonist (partial)	Agonist	–	i.a.	Agonist	Agonist (partial)	Agonist
BzATP	Agonist	i.a.	–	Agonist	Antagonist	i.a.	Agonist
2meSATP	Agonist	Agonist	–	Agonist	Agonist	i.a.	Agonist
Order of potency	ATP = 2meSATP > BzATP	2meSATP > ATP > BzATP		BzATP > 2meSATP > ATP	ATP = UTP = 2meSATP	UTP	ATP > 2meSATP > BzATP > UTP
Suramin	Antagonist	Antagonist	–	Antagonist (weak)	Antagonist (weak)	Antagonist (weak)	Antagonist
PPADS	Antagonist	Antagonist	–	Antagonist	i.a.	i.a.	i.a.
RB2	Antagonist	Antagonist	–	i.a.	Antagonist	Antagonist	i.a.
Order of potency	PPADS > RB2 = suramin	PPADS > suramin > RB2		PPADS >> suramin	RB2 >> suramin	RB2 > suramin	suramin

Agonist, potent agonist at rat P2 receptor orthologue; Agonist (partial), partial agonist at rat P2 receptor orthologue; i.a., inactive agonist at 100 μM; –, where the P2 receptor subtype functions poorly as a homomeric assembly and therefore agonist activity cannot be determined; Antagonist, potent antagonist at rat P2 receptor orthologue; Antagonist (weak), weak antagonist at rat P2 receptor orthologue where IC_{100} activity would be expected >1 mM.

© 2011 The Authors

17481716, 2011, 3, Downloaded from https://onlinelibrary.wiley.com/doi/10.1111/j.1748-1716.2011.02310.x by Northeastern Universitaet, Wiley Online Library on [10/07/2023]. See the Terms and Conditions (https://onlinelibrary.wiley.com/terms-and-conditions) on Wiley Online Library for rules of use; OA articles are governed by the applicable Creative Commons License

receptor subtypes are involved, based on the following (i) Extracellular ATP has activity at $P2X_{1,\ 3\ \text{and}\ 7}$ and $P2Y_{4\ \text{and}\ 11}$ receptors; however, given the potency of 2meSATP and BzATP, it is likely that the effects are predominantly mediated via 2meSATP-sensitive $P2X_1$ and BzATP-sensitive $P2X_7$ receptors (Table 1). (ii) In accordance, others have shown $P2X_7$ (determined pharmacologically)-evoked contraction of retinal pericytes (Kawamura *et al.* 2003), that $P2X_1$ is the most abundantly expressed P2 receptor on smooth muscle cells (Boarder & Hourani 1998), and to date there is little evidence for $P2X_3$ and $P2Y_{11}$ expression in the vasculature (Boarder & Hourani 1998). (iii) That ATP-evoked vasoconstriction is attenuated by suramin, PPADS and RB-2, and the effects of suramin and RB-2 are not additive, also indicates that both $P2X_1$ and $P2X_7$ receptors are involved. (iv) UTP is a full agonist at $P2X_3$ and $P2Y_{4\ \text{and}\ 11}$ receptors, however, as UTP-evoked vasoconstriction is attenuated by suramin and RB-2, but not by PPADS, suggests involvement of $P2Y_4$ receptors (Table 1) (Bogdanov *et al.* 1998). (v) In support, others have demonstrated that smooth muscle $P2Y_4$ receptor activation results in constriction of cerebral arterioles (Horiuchi *et al.* 2001).

The involvement of $P2X_3$ receptors or $P2Y_{6\ \text{or}\ 11}$ receptors cannot be completely dismissed, but given the information above it is unlikely that these receptors are major players in pericyte-mediated vasoconstriction of the vasa recta. In addition, the possibility exists that P2X receptor heteromeric assemblies involving $P2X_{1\ \text{or}\ 7}$ and $P2X_6$ subunits may be involved (e.g. predicted $P2X_{1/3\ \text{and/or}\ 1/6}$ assemblies) (Wildman & King 2008).

As to the identity of the P2 receptor(s) involved in pericyte-mediated vasodilation, it is difficult to comment beyond the receptor(s) is antagonized by suramin and PPADS, and insensitive to RB-2, and therefore we suggest $P2X_7$ involvement (Table 1). We appreciate the antagonists used in this study are not highly selective and thus conclusions drawn here are based on a summation of our experimental evidence, including both agonist and antagonist data, in addition to our RT-qPCR findings and also taking into account other experimental evidence available in the relevant literature. The current lack of selective P2 antagonists prevents us making more accurate conclusions at this stage.

Is the kidney slice model appropriate for studying tubulovascular cross-talk?

In summary, we have used the live kidney slice model to demonstrate pericyte-mediated regulation of *in situ* vasa recta diameter by extracellular nucleotides. Moreover, using P2 receptor antagonists we reveal the role of endogenous ATP in determining basal vasa recta tone and suggest tubular epithelial cells are the source of this endogenous ATP. That this model provides a setting in which vessels are in close proximity to tubular epithelial cells, so that this hypothesis can be further investigated, reinforces the potential of the live kidney slice model for investigating tubulovascular cross-talk.

Conflict of interest

None.

Experimental work was supported by The Medical Research Council (MRC; UK), The Wellcome Trust (UK) and St Peter's Trust for Kidney, Bladder and Prostate Research (UK).

References

Boarder, M.R. & Hourani, S.M. 1998. The regulation of vascular function by P2 receptors: multiple sites and multiple receptors. *Trends Pharmacol Sci* **19**, 99–107.

Bodin, P., Bailey, D. & Burnstock, G. 1991. Increased flow-induced ATP release from isolated vascular endothelial cells but not smooth muscle cells. *Br J Pharmacol* **103**, 1203–1205.

Bogdanov, Y.D., Wildman, S.S., Clements, M.P., King, B.F. & Burnstock, G. 1998. Molecular cloning and characterization of rat P2Y4 nucleotide receptor. *Br J Pharmacol* **124**, 428–430.

Burnstock, G. & Knight, G.E. 2004. Cellular distribution and functions of P2 receptor subtypes in different systems. *Int Rev Cytol* **240**, 31–304.

Crawford, C., Desai, T.D. & Peppiatt-Wildman, C.M. 2009. Validation of kidney slices as a viable model for studying *in situ* pericyte regulation of vasa recta capillaries in the renal medulla. *FASEB J* **23**, 804.17.

Das, A., Frank, R.N., Weber, M.L., Kennedy, A., Reidy, C.A. & Mancini, M.A. 1988. ATP causes retinal pericytes to contract *in vitro*. *Exp Eye Res* **46**, 349–362.

Dietrich, H.H., Kajita, Y. & Dacey, R.G., Jr. 1996. Local and conducted vasomotor responses in isolated rat cerebral arterioles. *Am J Physiol* **271**, H1109–H1116.

Epstein, F.H. 1985. Hypoxia of the renal medulla. *Q J Med* **57**, 807–810.

Erlinge, D. & Burnstock, G. 2008. P2 receptors in cardiovascular regulation and disease. *Purinergic Signal* **4**, 1–20.

Frank, R.N., Dutta, S. & Mancini, M.A. 1987. Pericyte coverage is greater in the retinal than in the cerebral capillaries of the rat. *Invest Ophthalmol Vis Sci* **28**, 1086–1091.

Fredholm, B.B., Chern, Y., Franco, R. & Sitkovsky, M. 2007. Aspects of the general biology of adenosine A2A signaling. *Prog Neurobiol* **83**, 263–276.

Holz, F.G. & Steinhausen, M. 1987. Renovascular effects of adenosine receptor agonists. *Ren Physiol* **10**, 272–282.

Horiuchi, T., Dietrich, H.H., Tsugane, S. & Dacey, R.G., Jr. 2001. Analysis of purine- and pyrimidine-induced vascular responses in the isolated rat cerebral arteriole. *Am J Physiol Heart Circ Physiol* **280**, H767–H776.

Jans, D., Srinivas, S.P., Waelkens, E., Segal, A., Lariviere, E., Simaels, J. & Van Driessche, W. 2002. Hypotonic treatment

© 2011 The Authors

evokes biphasic ATP release across the basolateral membrane of cultured renal epithelia (A6). *J Physiol* **545**, 543–555.

Kawamura, H., Sugiyama, T., Wu, D.M., Kobayashi, M., Yamanishi, S., Katsumura, K. & Puro, D.G. 2003. ATP: a vasoactive signal in the pericyte-containing microvasculature of the rat retina. *J Physiol* **551**, 787–799.

King, B.F. & Townsend-Nicholson, A. 2003. Nucleotide and nucleoside receptors. *Tocris Reviews* **23**, 1–12.

Kreisberg, M.S., Silldorff, E.P. & Pallone, T.L. 1997. Localization of adenosine-receptor subtype mRNA in rat outer medullary descending vasa recta by RT-PCR. *Am J Physiol* **272**, H1231–H1238.

Krogh, A. 1929. *The Anatomy and Physiology of Capillaries*. Yale University Press, New Haven.

Lin, S.L., Kisseleva, T., Brenner, D.A. & Duffield, J.S. 2008. Pericytes and perivascular fibroblasts are the primary source of collagen-producing cells in obstructive fibrosis of the kidney. *Am J Pathol* **173**, 1617–1627.

Loesch, A., Unwin, R., Gandhi, V. & Burnstock, G. 2009. Sympathetic nerve varicosities in close apposition to basolateral membranes of collecting duct epithelial cells of rat kidney. *Nephron Physiol* **113**, p15–p21.

Metea, M.R. & Newman, E.A. 2006. Glial cells dilate and constrict blood vessels: a mechanism of neurovascular coupling. *J Neurosci* **26**, 2862–2870.

O'Connor, P.M., Kett, M.M., Anderson, W.P. & Evans, R.G. 2006. Renal medullary tissue oxygenation is dependent on both cortical and medullary blood flow. *Am J Physiol Renal Physiol* **290**, F688–F694.

Pallone, T.L. & Huang, J.M. 2002. Control of descending vasa recta pericyte membrane potential by angiotensin II. *Am J Physiol Renal Physiol* **282**, F1064–F1074.

Pallone, T.L. & Silldorff, E.P. 2001. Pericyte regulation of renal medullary blood flow. *Exp Nephrol* **9**, 165–170.

Peppiatt, C.M., Howarth, C., Mobbs, P. & Attwell, D. 2006. Bidirectional control of CNS capillary diameter by pericytes. *Nature* **443**, 700–704.

Praetorius, H.A., Frokiaer, J. & Leipziger, J. 2005. Transepithelial pressure pulses induce nucleotide release in polarized MDCK cells. *Am J Physiol Renal Physiol* **288**, F133–F141.

Schwiebert, E.M. & Zsembery, A. 2003. Extracellular ATP as a signaling molecule for epithelial cells. *Biochim Biophys Acta* **1615**, 7–32.

Seldin, D.W. & Geibisch, G. 2008. Extracellular nucleotides and renal function. In: R.J. Alpern & S.C. Hebert (eds) *The Kidney: Physiology and Pathophysiology*, 4th edn, pp. 425–442. Elsevier, London.

Shepro, D. & Morel, N.M. 1993. Pericyte physiology. *FASEB J* **7**, 1031–1038.

Silldorff, E.P., Kreisberg, M.S. & Pallone, T.L. 1996. Adenosine modulates vasomotor tone in outer medullary descending vasa recta of the rat. *J Clin Invest* **98**, 18–23.

Sims, D.E. 1986. The pericyte – a review. *Tissue Cell* **18**, 153–174.

Sprague, R.S., Ellsworth, M.L., Stephenson, A.H. & Lonigro, A.J. 1996. ATP: the red blood cell link to NO and local control of the pulmonary circulation. *Am J Physiol* **271**, H2717–H2722.

Tilton, R.G., Kilo, C. & Williamson, J.R. 1979. Pericyte-endothelial relationships in cardiac and skeletal muscle capillaries. *Microvasc Res* **18**, 325–335.

Vassort, G. 2001. Adenosine 5′-triphosphate: a P2-purinergic agonist in the myocardium. *Physiol Rev* **81**, 767–806.

Wildman, S.S. & King, B.F. 2008. P2X receptors: epithelial ion channels and regulators of salt and water transport. *Nephron Physiol* **108**, p60–p67.

Wildman, S.S., Brown, S.G., Rahman, M., Noel, C.A., Churchill, L., Burnstock, G., Unwin, R.J. & King, B.F. 2002. Sensitization by extracellular Ca(2+) of rat P2X(5) receptor and its pharmacological properties compared with rat P2X(1). *Mol Pharmacol* **62**, 957–966.

Wildman, S.S., Marks, J., Turner, C.M., Yew-Booth, L., Peppiatt-Wildman, C.M., King, B.F., Shirley, D.G., Wang, W. & Unwin, R.J. 2008. Sodium-dependent regulation of renal amiloride-sensitive currents by apical P2 receptors. *J Am Soc Nephrol* **19**, 731–742.

Supporting Information

Additional Supporting Information may be found in the online version of this article:

Figure S1. Identification of pericytes on vasa recta capillaries. *Vasa recta* were labelled with Alexa-488-conjugated IB_4 (A, green) in fixed kidney slices. Pericyte cell body (arrowheads) and processes (arrows) can be seen when labelled with anti-NG2 and probed with an Alexa-555-conjugated secondary antibody (B, red). An overlay of images (A) and (B) identifies pericytes (red) at regular intervals along vasa recta capillaries (green) (C).

Movie S1. Effect of bath-applied ATP (100 μM) on *in situ* (subsurface) vasa recta diameter. Reversible ATP-evoked vasoconstriction is seen specifically at the highlighted pericyte site.

Table S1. Primer sequences and expected product sizes.

Please note: Wiley-Blackwell are not responsible for the content or functionality of any supporting materials supplied by the authors. Any queries (other than missing material) should be directed to the corresponding author for the article.

© 2011 The Authors

17481716, 2011, 3, Downloaded from https://onlinelibrary.wiley.com/doi/10.1111/j.1748-1716.2011.02310.x by Northeastern Universitaet, Wiley Online Library on [10/07/2023]. See the Terms and Conditions (https://onlinelibrary.wiley.com/terms-and-conditions) on Wiley Online Library for rules of use; OA articles are governed by the applicable Creative Commons License